A Morphological Study of Substorm-Associated Disturbances in the Ionosphere

C. G. PARK

Radioscience Laboratory, Stanford University, Stanford, California 94305

The whistler technique was used in an earlier study to observe a rapid depletion of the day side plasmasphere during isolated substorm activity on June 25, 1965 (Park, 1973). It was inferred that this depletion was due to dumping of plasma into the underlying ionosphere. The average downward flux was estimated to be of the order of 10^9 el/cm^2 s across the 1000-km level, large enough to cause significant enhancements in electron concentrations in the ionospheric F region. In this paper the ionospheric behavior during the same event is examined by using ionosonde data from some 40 stations in the northern hemisphere. The results show that the F_2 layer critical frequency f_oF_2 was enhanced up to 25% above the monthly median level in the same general area where downward fluxes were inferred from whistlers. This was followed by ~20% depressions in f_oF_2 the next day, when geomagnetic conditions were quiet. These substorm effects were observed in a wide range of latitude but were limited in local time and longitude. In the area affected, the ionospheric disturbance caused by this moderate substorm activity (~500 γ maximum AE index and ~6-hour duration) was similar in many respects to major worldwide ionospheric storms. These results support the view that ionospheric storms can be understood in terms of the superposed effects of many substorms.

The dynamical behavior of the plasmasphere-ionosphere system is strongly correlated with geomagnetic activity. Electric fields associated with magnetospheric substorms penetrate deep within the plasmasphere and cause large density variations through tube interchange motions and through modulations of coupling fluxes with the underlying ionosphere. Although these effects are more dramatic during major magnetic storms, isolated substorms afford better opportunities to study the spatial extent of the effects and to separate temporal and spatial variations. The whistler technique is particularly well suited for such studies, and a recent review paper on this subject was done by *Carpenter and Park* [1973].

The ionospheric F layer also responds to magnetospheric substorms. Several earlier papers have discussed vertical motions and accompanying density changes in the middle-latitude nighttime F layer [*Park*, 1971; *Park and Meng*, 1971, 1973]. These effects are believed to be the ionospheric counterpart of substorm-induced disturbances in the overlying plasmasphere. In this paper we will examine a substorm-induced disturbance in the day side ionosphere. There were disturbance signatures in both the ionosphere and the plasmasphere that can only be explained in terms of strong coupling between the two regions. The plasmasphere side of the picture was studied in detail by the whistler technique, and the results were reported separately [*Park*, 1973]. To summarize them briefly, whistlers recorded in Antarctica indicated a rapid depletion of the day side plasmasphere during substorm activity on June 25, 1965. It was inferred that this depletion was due to downward flow of plasma into the underlying ionosphere induced by westward electric fields. The average downward flux was estimated to be of the order of 10^9 el/cm^2 s. These results are consistent with simultaneous ionosonde observations of the F_2 layer reported in this paper.

The event discussed here involves relatively isolated substorm activity of moderate intensity (maximum Kp = 4o). Yet, the ionospheric disturbance associated with it is remarkably similar to behavior during major ionospheric storms [e.g., *Obayashi*, 1964; *Rishbeth*, 1968]. This suggests that ionospheric storms can be understood in terms of the superposed effects of substorms, just as geomagnetic storms are now understood in terms of magnetic substorms [*Akasofu*, 1968].

It is well known that ionospheric storm phenomena depend strongly on the season. In this paper we will limit our discussion to a case study based on summer hemisphere data only and note that the results obtained may not apply to other seasons. More discussion on this point will follow.

OBSERVATIONS AND INTERPRETATIONS

Geomagnetic data. Figure 1 shows geomagnetic indices AE, Kp, and Dst for the period June 14–26, 1965. A storm sudden commencement occurred near 1200 UT on June 15, followed by a main phase that lasted through June 17. This magnetic storm was accompanied by a typical worldwide ionospheric storm that lasted until June 18. There then followed a long period of extreme quiet until it was interrupted by relatively isolated substorm activity near 1430 UT on June 25. Although this event was moderate in both intensity and duration, it produced in certain parts of the world ionospheric disturbances very similar to those from the June 15 storm. The hatched bars at the top of Figure 1 indicate the duration of the ionospheric disturbances.

Figure 2 shows auroral zone magnetograms during the substorm activity on June 25, 1965. The activity started at ~1430 UT and lasted until ~2100 UT. It is likely that there were several overlapping substorms during this ~6-hour period. However, it is not possible to resolve individual substorms in magnetic records because of rapid motions of the auroral electrojet current system with respect to the recording stations. We will now examine ionospheric data during these disturbances.

Ionospheric data. Figure 3 compares the ionospheric behavior over Washington during the June 15 event (upper panel) with that of the June 25 event (lower panel). The dots are hourly values of f_oF_2 available through World Data Center A, and the solid curves represent the monthly median behavior. Similarities between the two events are apparent. In

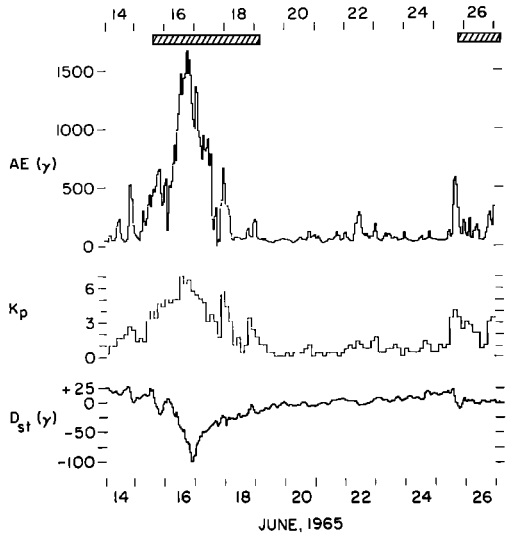

Fig. 1. Plots of auroral electrojet (*AE*) index, *Kp*, and *Dst* for the period June 14–26, 1965.

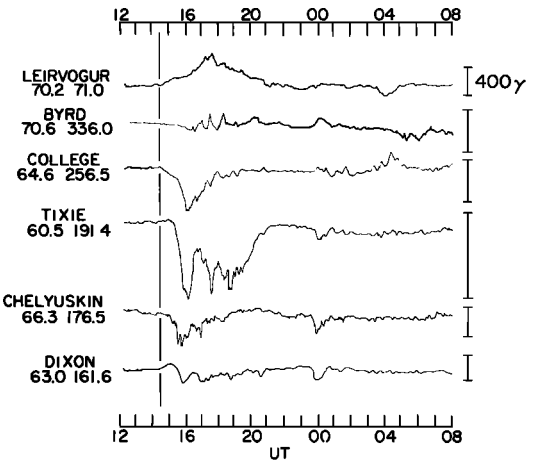

Fig. 2. Auroral zone magnetograms showing the substorm activity of interest in this paper. The vertical line indicates the approximate time of substorm onset.

the upper panel, f_oF_2 is enhanced on the first day of the storm main phase and depressed on subsequent days, except for sharp increases in the evening hours as long as the main phase continues. After the main phase is over, f_oF_2 remains depressed for another day before it fully recovers. This is typical storm behavior at Washington in the summer. The behavior shown in the lower panel is shorter in duration but otherwise remarkably similar to the storm behavior above. The recovery time following the disturbance and the magnitudes of peak enhancements and depressions in the two events are also similar.

An important difference is the fact that the disturbance was confined to a limited area during the June 25 event, whereas it was worldwide during the June 15 event. This can be clearly seen in the behavior of the ionosphere over Tomsk, illustrated in Figure 4. Here the June 15 storm produced signatures similar to those over Washington, but no clear sign of disturbance can be associated with the substorm activity on June 25. Figures 5–7 illustrate the spatial extent of the June 25 disturbance by using data from a network of ionosonde stations in the northern hemisphere. The station symbols and their coordinates are listed in Table 1. Figure 5*a* shows the ionospheric behavior over stations near the Washington meridian and covering 0°–70° geomagnetic latitude. A comparison with the June 15 storm data in Figure 5*b* shows that the two events produced similar disturbances in the entire latitude range, except at the equatorial station Huancayo. Figures 6 and 7 show middle-latitude data at different longitudes. In Figure 6 the stations are arranged from top to bottom by increasing longitudinal separation from the Washington meridian to the east, and in Figure 7, toward the west. It is clear that the substorm effects diminish rapidly in both directions away from the Washington meridian. Note that the stations that observed a large positive phase also observed a large negative phase following the substorm activity. The positive phase occurs during the substorm activity in a limited local time sector, which then defines an area where the subsequent negative phase is observed. This is illustrated in Figures 8–10.

In Figure 8, data from 39 ionosonde stations between 20° and 60° geomagnetic latitude in the northern hemisphere were used to obtain the local time distribution of the positive phase. We computed percentage deviation of hourly f_oF_2 values from the monthly median for each station between 1500 and 2000 UT. (Recall that the substorm activity lasted from ~1430 to ~2100 UT.) These percentages were then averaged over all applicable stations for each local time. The number of stations used for each local time is indicated at the

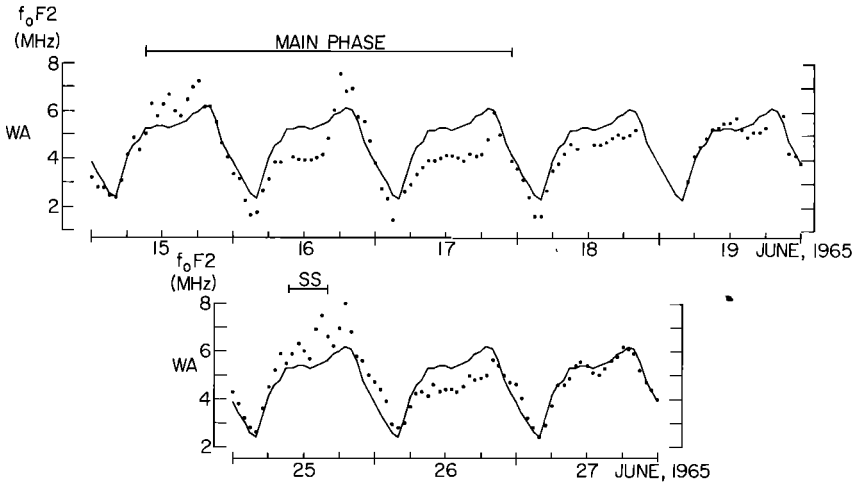

Fig. 3. Plots of f_oF_2 versus local time at Washington. The solid curves represent the monthly median behavior.

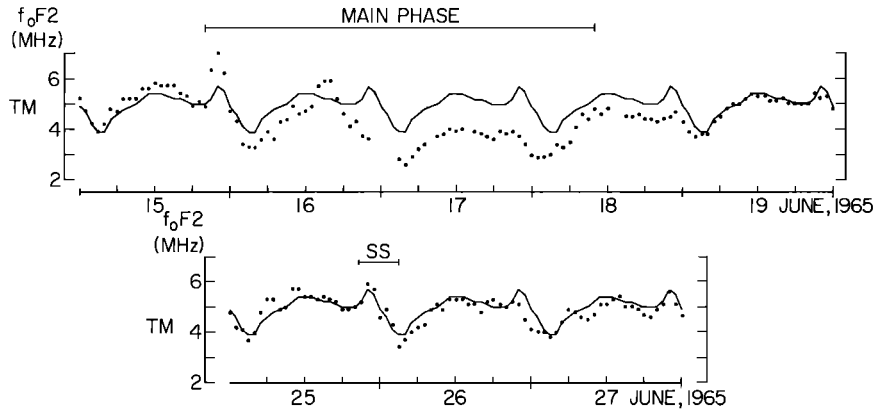

Fig. 4. Plots of f_0F_2 versus local time at Tomsk. The solid curves represent the monthly median behavior.

top of the figure. The averages based on fewer than four stations are shown as dashed lines. There is a prominent peak at 1500 LT and a secondary peak at 1900 LT. These two peaks may involve two different mechanisms, as will be discussed later.

Figure 9 illustrates the longitudinal dependence of the negative phase in middle latitudes. For each station shown in the figure the percentage deviation of f_0F_2 from the monthly median value was determined at 1100, 1200, and 1300 LT immediately following the substorm. Figure 9 shows a plot of the average of these three hourly values. There is a deep valley near the Washington meridian, rising steeply on both sides. It is contrasted sharply with a similar plot made in Figure 10 for the latitudinal profile near the Washington meridian. Here the magnitude of the percentage depression is remarkably constant with latitude from Bogota at 16° geomagnetic latitude to Churchill at 69° geomagnetic latitude.

Further details near Washington. We now examine in greater detail ionosonde and other related data, all from within a few hundred kilometers of Washington. These include true height analysis of ionosonde records from Wallops Island, electron columnar content deduced from Faraday rotation of VHF signals between the ATS 1 satellite and Hamilton, Massachusetts (the subsatellite point at 350-km altitude is 39°N and 70°W), and magnetic records from Fredericksburg.

Figure 11 shows the columnar content data for June 25–27. These data were kindly provided by J. Klobuchar and M.

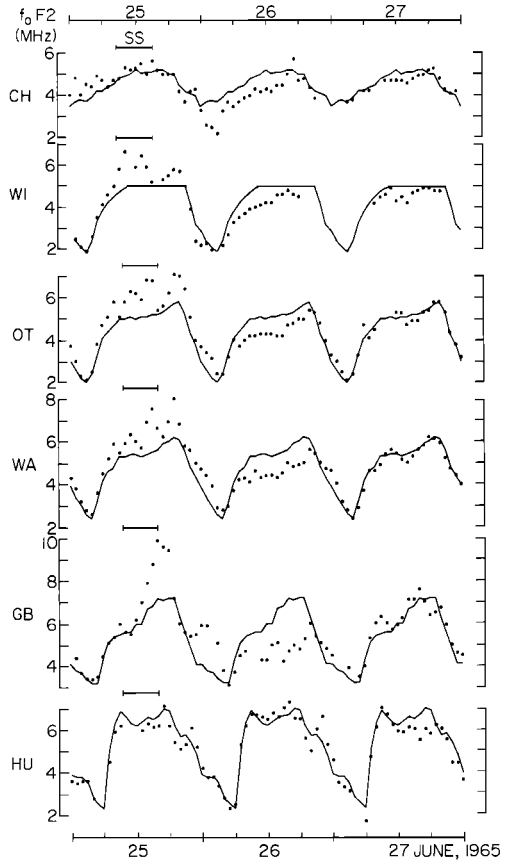

Fig. 5*a*. Plots of f_0F_2 versus local time at Churchill, Winnipeg, Ottawa, Washington, Grand Bahamas, and Huancayo for the period June 25–27, 1965. The horizontal bars indicate the approximate duration of the magnetic substorm activity. The solid curves represent the monthly median behavior.

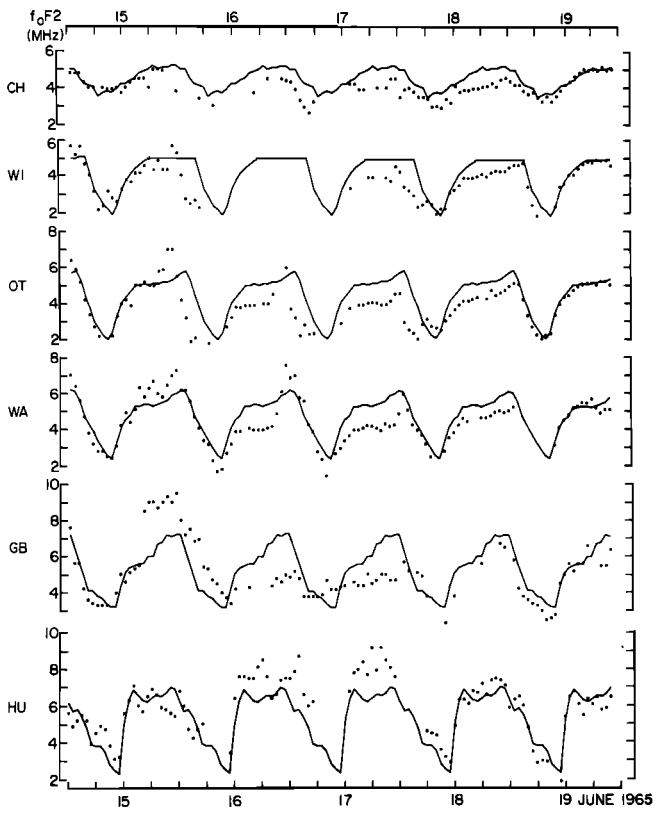

Fig. 5*b*. Plots similar to those in Figure 5*a* for the period June 15–19, 1965.

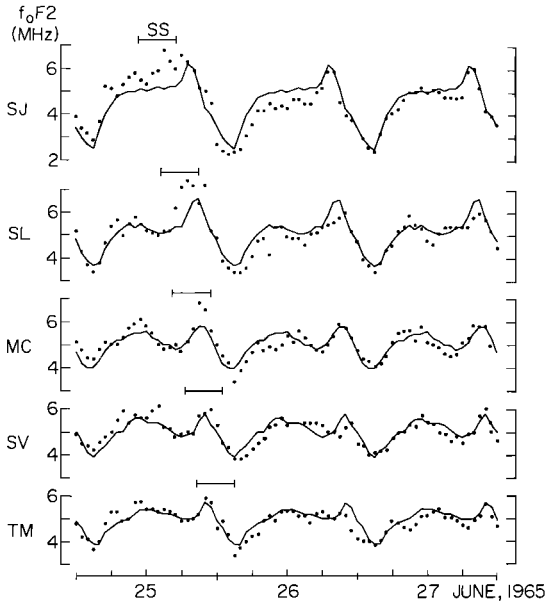

Fig. 6. Plots of f_0F_2 versus local time at St. Johns, Slough, Moscow, Sverdlovsk, and Tomsk. The solid curves represent the monthly median behavior, and the horizontal bars indicate the approximate duration of the magnetic substorm activity.

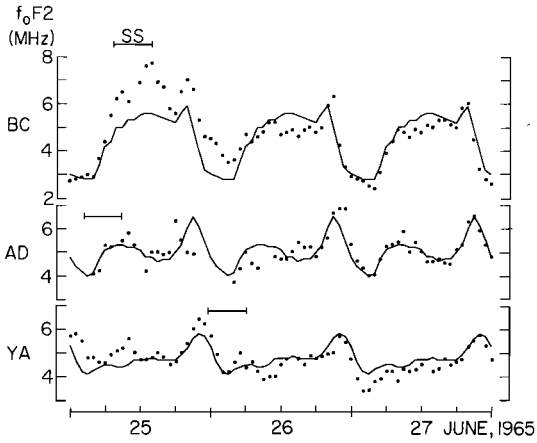

Fig. 7. Plots of f_0F_2 versus local time at Boulder, Adak, and Yakutsk. The solid curves represent the monthly median behavior, and the horizontal bars indicate the approximate duration of the magnetic substorm activity.

Mendillo. The dashed curve, shown here for reference, was obtained by averaging the data for the previous 4 days, when the geomagnetic condition was extremely quiet. The columnar content curve shows variations similar to f_0F_2 over Washington (see Figure 3). Therefore it is clear that the observed behavior of f_0F_2 cannot be explained by redistribution of plasma within the ionosphere.

The height variations of the F_2 layer peak provide some further insight into the substorm dynamics. Figure 12 shows plots of N_mF_2 and h_mF_2 deduced from true height analysis of Wallops Island ionograms. True heights were calculated with the aid of a computer program written by D. Bubenik of our laboratory, who adopted the procedures developed by *Paul* [1967], *Howe and McKinnis* [1967], and *Wright* [1967]. The curves represent the monthly average behavior based on composite $N(h)$ profiles available from World Data Center A. An important point in the figure is the fact that h_mF_2 does not track N_mF_2. In fact, there is a tendency for h_mF_2 to decrease when N_mF_2 increases, and vice versa. It is clear that the observed variations in N_mF_2 cannot be explained simply as the result of the layer moving up or down to regions of different recombination losses. Coupling fluxes with the overlying plasmasphere must be an important factor. Note that between 1800 and 2000 UT, N_mF_2 increases, while the F_2 layer peak is lowered to regions of increasing recombination losses. This requires an additional source of ionization, which is believed to be the overlying plasmasphere.

A qualitative interpretation of Figure 12 is as follows. A westward electric field associated with the substorm tends to lower the ionosphere through $\mathbf{E} \times \mathbf{B}$ drift. This alters the coupling conditions between the ionosphere and the plasmasphere and induces downward flow of ionization by a

TABLE 1. A List of Ionosonde Stations

Station	Symbol	Geographic Coordinates		Geomagnetic Coordinates	
		°N	°E	°N	°E
Adak	AD	51.9	183.4	47.2	240.0
Bogota	BO	4.5	285.8	16.0	354.6
Boulder	BC	40.0	264.7	48.9	316.4
Churchill	CH	58.8	265.9	68.7	322.8
Grand Bahamas	GB	26.6	281.8	37.9	349.6
Huancayo	HU	−12.0	284.7	−0.6	353.8
Irkutsk	IR	52.5	104.0	41.1	174.4
Leningrad	LG	60.0	30.7	56.3	117.4
Lindau	LI	51.6	10.1	52.3	93.9
Mexico City	MX	19.4	260.3	29.2	326.5
Moscow	MC	55.5	37.3	50.9	120.5
Ottawa	OT	45.4	284.1	56.8	351.1
Rostov	RO	47.2	309.7	42.5	119.2
Slough	SL	51.5	359.4	54.4	83.3
St. Johns	SJ	47.6	307.3	58.5	21.2
Sverdlovsk	SV	56.7	61.1	48.5	140.7
Tomsk	TM	56.5	84.9	45.9	159.6
Wallops Island	WP	37.9	284.5	49.3	352.1
Washington	WA	38.7	282.9	50.1	350.1
Winnipeg	WI	49.8	265.6	59.9	326.6
Yakutsk	YA	62.0	129.6	50.9	193.8

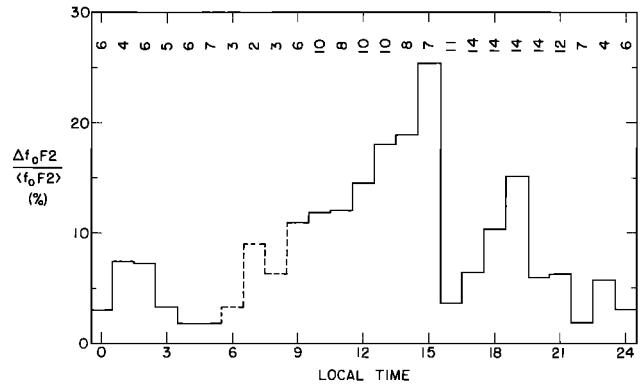

Fig. 8. A histogram showing percentage deviation of f_0F_2 from the monthly median as a function of local time during the period 1500–2000 UT, June 25, 1965. Data from 39 stations between 20° and 60°N geomagnetic latitude were used. The number of stations used to obtain the average percent deviation for each local time hour is shown at the top. Dashed line represents averages based on fewer than four stations.

mechanism discussed elsewhere [*Park*, 1971, 1973]. When this flux is large enough to overcome the increased recombination losses, we see enhancements in f_0F_2. Quantitative interpretation is difficult because the resulting behavior of N_mF_2 and h_mF_2 involves several competing processes. The influx of plasma competes with increased losses in controlling N_mF_2 as the layer is lowered. The tendency for a westward electric field to lower h_mF_2 is opposed by ion drag effects as well as by downward coupling fluxes, which tend to raise h_mF_2. Time-varying electric fields add to the complexity. An attempt is being made to study these effects theoretically by using numerical techniques, and preliminary results give support to the qualitative interpretation above.

Other evidence for a westward electric field comes from middle-latitude magnetograms. The D component magnetogram from Fredericksburg is shown at the bottom of Figure 12. If we assume that the magnetic deflection is caused by overhead ionospheric currents (a reasonable assumption on the day side, but not on the night side) and if we assume a height-integrated Hall conductivity of 10 mhos, a westward electric field of ~8 mV/m can be deduced from the 50-γ westward magnetic deflection observed at Fredericksburg.

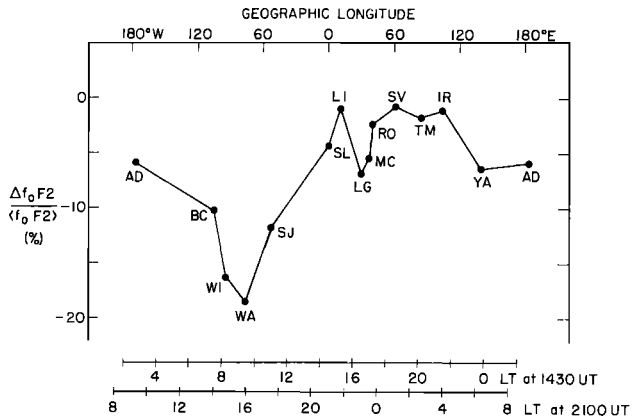

Fig. 9. A plot of percentage deviation of f_0F_2 from the monthly median at northern hemisphere middle-latitude stations. The data points were obtained by averaging over the hourly values at 1100, 1200, and 1300 LT on June 26, 1965, at each station. Station symbols and their coordinates are listed in Table 1. The two horizontal scales at the bottom show local time at 1430 and 2100 UT, the approximate times of the beginning and end of the magnetic substorm activity.

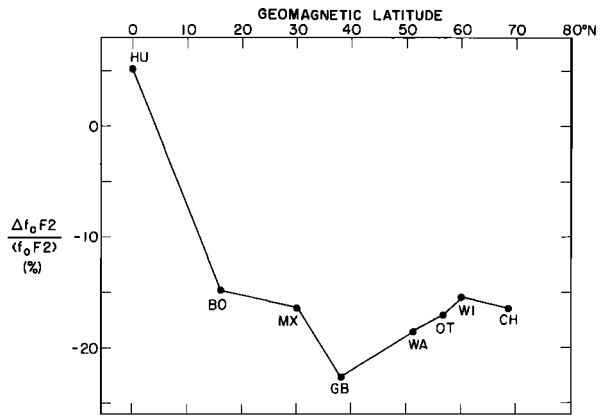

Fig. 10. A plot similar to that in Figure 9 but against geomagnetic latitude for stations near the Washington meridian.

Whistler observations. The substorm activity on June 25 produced dramatic effects on the plasmasphere, as was reported earlier [*Park*, 1973]. The plasmasphere observations were made with whistlers recorded in Antarctica and North America within ~±30° of the Washington meridian. We will briefly summarize the whistler results relevant to this paper.

The long period of quiet geomagnetic conditions prior to the substorm event allowed the plasmasphere to reach a relatively large size and density level by filling from the underlying ionosphere. Immediately following the substorm, electron density in parts of the plasmasphere was reduced to approximately half the presubstorm level. This was interpreted as being the result of localized draining of the plasmasphere by downward flow of plasma into the ionosphere. Figure 13 summarizes the results in terms of electron tube content, which is defined as the total number of electrons in a tube of magnetic flux with 1-cm² cross-sectional area at 1000-km altitude and extending to the magnetic equator. The two curves in the upper panel represent tube content profiles before and after the substorm event. It was inferred from detailed studies of whistler records that the change from the 'before' profile to the 'after' profile was brought about by a combination of inward convection of plasma and draining through the underlying ionosphere. This is illustrated in the bottom panel of Figure 13.

The electric field strength required for the inward convection as shown was estimated to be of the order of 1 mV/m in the equatorial plane [*Park*, 1973]. This compares well with ~8 mV/m at ionospheric heights estimated from the magnetogram. It was also possible to infer from whistlers that the downward flow of plasma occurred in a limited local time sector and that the average flux during the substorm was of the order of 10^9 el/cm² s across the 1000-km level. The area of inferred downward fluxes is roughly the same as that of the large positive phase in the ionospheric F region shown in this paper.

DISCUSSION

The results of this study indicate that substorm effects in the ionosphere are strongly local time dependent. During major storms these effects become worldwide because all stations have sufficient time to go through all local time sectors while substorm activity (or the main phase of the storm) is in progress. It is an important task to learn in detail how the ionosphere-plasmasphere system responds to isolated magnetospheric substorms as a function of local time. It is

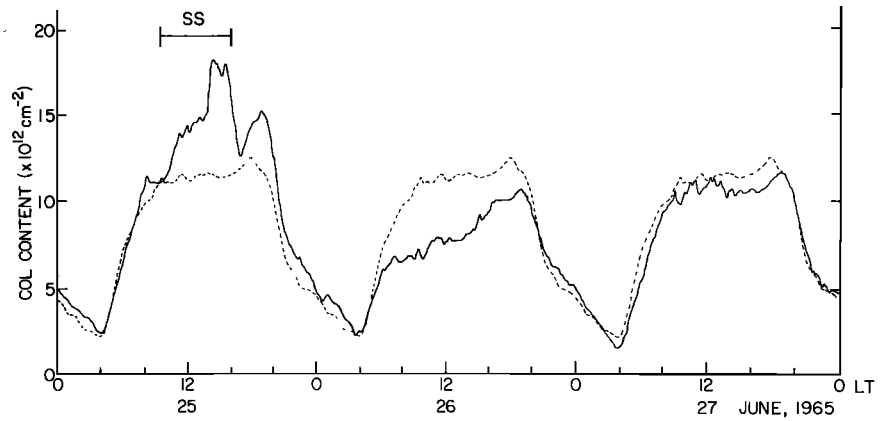

Fig. 11. A plot of electron columnar content deduced from Faraday rotation of VHF signals from ATS 1 satellite to Hamilton, Massachusetts. The dashed curve represents the average behavior during the previous 4 quiet days, June 21–24, 1965. (Courtesy of J. Klobuchar and M. Mendillo, Air Force Cambridge Research Laboratory.)

likely that different mechanisms are operative in different local time sectors.

In the previous section, emphasis was placed on enhancements in f_oF_2 that are believed to be caused by an influx of ionization from the plasmasphere. Another mechanism for enhanced f_oF_2 involves an eastward electric field that lifts the F_2 layer to higher altitudes, where recombination losses are smaller [*Evans*, 1970]. This may be the same eastward electric field that is believed to 'peel off' the plasmasphere in the evening sector and form 'detached' plasma regions [*Chappell et al.*, 1971]. It is possible that this mechanism is responsible for the secondary peak in $\Delta f_oF_2/(f_oF_2)$ centered at 1900 LT (see Figure 8), although we cannot provide evidence for it in this paper.

The negative phase of the ionospheric disturbance was centered near the Washington meridian, where it lasted throughout the daylight hours on June 26. Since geomagnetic conditions were quiet during this time, it is not likely that electric fields were involved. It was shown in earlier papers [*Park*, 1970, 1973] that upward fluxes into the protonosphere could not be responsible for such depressions in f_oF_2. It is then most likely that heating of the neutral atmosphere and resulting changes in composition are responsible for the negative phase. Such effects have been discussed by a number of authors [*Obayashi and Matuura*, 1972; *Mayr and Volland*, 1973; *Chandra and Herman*, 1969]. The heating probably occurred during the substorm activity on June 25. It then required about a day for cooling. If this interpretation is correct, the heat source must have been limited in local time but must have penetrated to low latitudes without suffering much attenuation (see Figures 9 and 10). Heating by electric fields, as discussed by *Cole* [1971], appears to be one possibility.

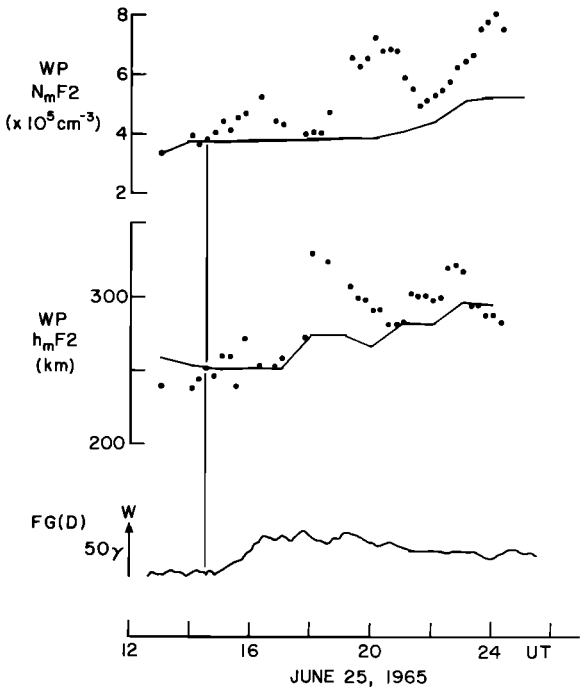

Fig. 12. Plots of the F_2 layer peak density N_mF_2 and the height of the peak h_mF_2 deduced from true height analysis of Wallops Island ionograms. The bottom trace is a transcription of the D component magnetogram from Fredericksburg. The arrow indicates a 50-γ deflection in the westerly direction. The vertical line shows the approximate substorm onset time.

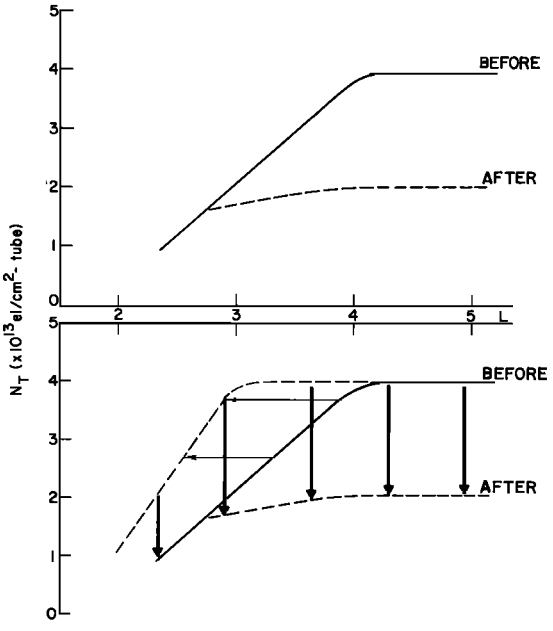

Fig. 13. A sketch summarizing whistler observations of the plasmasphere reported by *Park* [1973]. The top panel shows tube content in the plasmasphere as a function of L before and after the substorm on June 25, 1965. The bottom panel shows schematically how an inward convection combined with downward flow of plasma along field lines into the underlying ionosphere may have changed the tube content profile.

A question may be raised as to the repeatability or predictability of the substorm effects described here. This can be answered only through a large number of case studies. Magnetospheric substorms vary widely in intensity, duration, location of the epicenter, etc. In addition, the response of the ionosphere to a given magnetospheric substorm depends on the state of the neutral atmosphere and therefore on season, sunspot cycle, etc. The initial states of the magnetosphere and the ionosphere are probably also important. As an example of the seasonal dependence, the substorm effects described in this paper for the summer hemisphere were totally absent in the simultaneous winter hemisphere data. In spite of these complicating factors, a preliminary survey of substorms has revealed a number of cases similar to the one reported here. Thus it can be stated that the phenomena reported here are repeatable under certain circumstances, although these circumstances cannot be specified precisely at this stage of research.

CONCLUSIONS

Magnetospheric substorms involving a maximum AE index of only ~ 500 γ can produce large disturbances in the ionospheric F region, comparable in magnitude to major ionospheric storms. The substorm effects are widespread in latitude but limited in local time and longitude. This suggests that worldwide ionospheric storms can be understood in terms of the superposed effects of many substorms occurring over a period of a day or longer. Transverse electric fields and the flow of thermal plasma between the ionosphere and the plasmasphere are important for the substorm behavior of both regions. These results emphasize the value of studying the coupled ionosphere-plasmasphere system during isolated substorms.

Acknowledgments. I wish to thank C.-I. Meng for helpful discussions, D. L. Carpenter for many helpful comments on the manuscript, and D. Wiggin for helping with data analysis. I also wish to thank D. Bubenik for making available to me his computer program for true height analysis of ionograms. The ionospheric and geomagnetic data used in this study were made available through World Data Center A. This research was sponsored by the Atmospheric Sciences Section of the National Science Foundation under grants GA-28042 and GA-32590X. The computing facilities at Stanford University were sponsored in part by the Office of Computer Sciences of the National Science Foundation under grant GP-948.

* * *

The Editor thanks T. Obayashi and another referee for their assistance in evaluating this paper.

REFERENCES

Akasofu, S.-I., *Polar and Magnetospheric Substorms*, p. 2, D. Reidel, Dordrecht, Netherlands, 1968.

Carpenter, D. L., and C. G. Park, On what ionospheric workers should know about the plasmapause-plasmasphere, *Rev. Geophys. Space Phys., 11,* 133, 1973.

Chandra, S., and J. R. Herman, F region ionization and heating during magnetic storms, *Planet. Space Sci., 17,* 841, 1969.

Chappell, C. R., K. K. Harris, and G. W. Sharp, The day side of the plasmasphere, *J. Geophys. Res., 76,* 7632, 1971.

Cole, K. D., Electrodynamic heating and movement of the thermosphere, *Planet. Space Sci., 19,* 59, 1971.

Evans, J. V., The June 1965 magnetic storm: Millstone Hill observations, *J. Atmos. Phys., 32,* 1629–1640, 1970.

Howe, H. H., and D. E. McKinnis, Ionospheric electron density profiles with continuous gradients and underlying ionization corrections, 2, Formulation for a digital computer, *Radio Sci., 2,* 1135, 1967.

Mayr, H. G., and H. Volland, Magnetic storm characteristics of the thermosphere, *J. Geophys. Res., 78,* 2251, 1973.

Obayashi, T., Morphology of storms in the ionosphere, in *Research in Geophysics,* vol. 1, *Sun, Upper Atmosphere and Space,* edited by H. Odishaw, p. 335, MIT Press, Cambridge, Mass., 1964.

Obayashi, T., and N. Matuura, Theoretical model of F region storms, in *Solar Terrestrial Physics/1970,* edited by E. R. Dyer, p. 199, D. Reidel, Dordrecht, Netherlands, 1972.

Park, C. G., A whistler study of the interchange of ionization between the ionosphere and the protonosphere, *Tech. Rep. 3442-1,* Radioscience Lab., Stanford Univ., Stanford, Calif., Aug. 1970.

Park, C. G., Westward electric fields as the cause of nighttime enhancements in electron concentrations in mid-latitude F region, *J. Geophys. Res., 76,* 4560, 1971.

Park, C. G., Whistler observations of the depletion of the plasmasphere during a magnetospheric substorm, *J. Geophys. Res., 78,* 672, 1973.

Park, C. G., and C.-I. Meng, Vertical motions of the mid-latitude F_2 layer during magnetospheric substorms, *J. Geophys. Res., 76,* 8326, 1971.

Park, C. G., and C.-I. Meng, Distortions of the night side ionosphere during magnetospheric substorms, *J. Geophys. Res., 78,* 3828, 1973.

Paul, A. K., Ionospheric electron density profiles with continuous gradients and underlying ionization corrections, 1, The mathematical-physical problem of real height determination from ionograms, *Radio Sci, 2,* 1127, 1967.

Rishbeth, H., On explaining the behavior of the F region, *Rev. Geophys. Space Phys., 6,* 33, 1968.

Wright, J. W., Ionospheric electron density profiles with continuous gradients and underlying ionization corrections, 3, Practical procedures and some instructive examples, *Radio Sci., 2,* 1159, 1967.

(Received November 30, 1973;
accepted April 22, 1974.)